Published by Institute of Physics Publishing for SISSA
Received: *February 24, 2005*
Revised: *May 21, 2005*
Accepted: *June 12, 2005*
Published: *July 5, 2005*

# Superradiant instabilities of rotating black branes and strings

**Vitor Cardoso**
*McDonnell Center for the Space Sciences, Department of Physics*
*Washington University, St. Louis, Missouri 63130, U.S.A., and*
*Centro de Física Computacional, Universidade de Coimbra*
*P–3004–516 Coimbra, Portugal*
*E-mail:* vcardoso@wugrav.wustl.edu

**Shijun Yoshida**
*Science and Engineering, Waseda University*
*Okubo, Shinjuku, Tokyo 169-8555, Japan*
*E-mail:* shijun@waseda.jp

Abstract: Black branes and strings are generally unstable against a certain sector of gravitational perturbations. This is known as the Gregory-Laflamme instability. It has been recently argued [1, 2] that there exists another general instability affecting many rotating extended black objects. This instability is in a sense universal, in that it is triggered by any massless field, and not just gravitational perturbations. Here we investigate this novel mechanism in detail. For this instability to work, two ingredients are necessary: (i) an ergo-region, which gives rise to superradiant amplification of waves, and (ii) "bound" states in the effective potential governing the evolution of the particular mode under study. We show that the black brane $\mathrm{Kerr}_4 \times R^{\mathrm{p}}$ is unstable against this mechanism, and we present numerical results for instability timescales for this case. On the other hand, and quite surprisingly, black branes of the form $\mathrm{Kerr}_{\mathrm{d}} \times R^{\mathrm{p}}$ are all stable against this mechanism for $\mathrm{d} > 4$. This is quite an unexpected result, and it stems from the fact that there are no stable circular orbits in higher dimensional black hole spacetimes, or in a wave picture, that there are no bound states in the effective potential. We also show that it is quite easy to simulate this instability in the laboratory with acoustic black branes.

Keywords: p-branes, Black Holes in String Theory, Black Holes.

## Contents





## 1. Introduction

We are all painfully aware that exact, closed form solutions to physical problems are an exception. The rule is that one must resort to all kinds of tricks and assumptions in order to get a grip on the equations: this is why, despite their little insight into the physics, numerical solutions are proliferating as problems become more and more complex. Exact solutions are therefore most welcome. Exact solutions to Einstein equations are extremely useful, especially if they describe simple yet physically attainable systems. Indeed, take for example the famous Schwarzschild metric: with this exact solution at hand, describing the geometry outside a spherically symmetric distribution of matter, one was able to compute the deflection of light as it passes near the Sun (and to match the theoretical prediction against the observational data), thereby giving strong support to Einstein's theory. We now know that the outside geometry of many astrophysical objects is well described by the Schwarzschild metric, and we can start studying them by investigating the properties of this metric.

One of the most important things that one should study first is the classical stability of a given solution: if a solution is unstable, then it most certainly will not be found in nature (unless the instability is secular) and the solution loses most of its power. What does one mean by stability? In this classical context, stability means that a given initially bounded perturbation of the spacetime remains bounded for all times. For example, the Schwarzschild spacetime is stable against all kinds of perturbations, massive or massless [3]. Thus, if one considers small deviations from the Schwarzschild geometry (for instance throwing a small stone into the black hole, this disturbs the geometry), stability means that these small perturbations eventually fade away. They will never disrupt the spacetime. The term "perturbations" means either small (metric) deviations in the geometry or small-amplitude fields in the geometry, for example scalar fields or electromagnetic fields (as such, deviations in the geometry can be looked at as perturbations induced by gravitons). So, the Schwarzschild geometry is indeed appropriate to study astrophysical objects.

Here we shall investigate an instability which is rotation-triggered, and which was hinted at for the first time by Marolf and Palmer [1]. The mechanism has recently been explained in [2], where it was shown that it could be triggered in many systems. However, a detailed description is still lacking, and this is the main purpose of the present work. The physical nature of this instability can be understood with the following facts: It is known that the Kerr geometry displays superradiance [4]. This means that in a scattering experiment of a wave with frequency $\omega < m\Omega$ ($m$ is again the azimuthal wave quantum number) the scattered wave will have a larger amplitude than the incident wave, the excess energy being withdrawn from the object's rotational energy. Now suppose that one encloses the rotating black hole inside a spherical mirror. Any initial perturbation will get successively amplified near the black hole event horizon and reflected back at the mirror, thus creating an instability. This is the black hole bomb, as devised in [5] and recently improved in [6]. This instability is caused by the mirror, which is an artificial wall, but one can devise natural mirrors if one considers massive fields [7, 8]. Imagine a wavepacket of the massive field in a distant circular orbit. The gravitational force binds the field and keeps it from escaping or radiating away to infinity. But at the event horizon some of the field goes down the black hole, and if the frequency of the field is in the superradiant region then the field is amplified. Hence the field is amplified at the event horizon while being bound away from infinity. Yet another way to understand this, is to think in terms of wave propagation in an effective potential. If the effective potential has a well, then waves get "trapped" in the well and amplified by superradiance, thus triggering an instability. In the case of massive fields on a (four-dimensional) Kerr background, the effective potential indeed has a well. Consequently, the massive field grows exponentially and is unstable. It is the presence of a bound state that simulates the mirror, and without a bound state we should never get an instability.

Now, consider for example the following rotating black-brane geometry

$$ds^2 = ds^2_{\rm Kerr} + dx^i dx_i \,, \tag{1.1}$$

where Kerr stands for the usual Kerr geometry. It's a known property, and we will show it explicitly, that the propagation of a *massless* field (scalar, electromagnetic, or gravitational) in this *black-brane* geometry, is *equivalent* to the propagation of a *massive* field in the vicinity of the Kerr *black hole*. Thus, the particular black brane (1.1) is unstable.

The instability argument applies to many rotating extended objects, and here we shall study some of them, making an extensive analysis of the d−dimensional case (1.1). We show that for $\mathrm{d}=4$ they are unstable, and we present detailed results on the stability. For $\mathrm{d}>4$ the black branes described by

$$ds^2 = ds^2_{\mathrm{Kerr_d}} + dx^i dx_i\,, \tag{1.2}$$

are stable, where $\mathrm{Kerr_d}$ is the Myers-Perry [9] rotating black hole. This is due to the non-existence of stable bound orbits for massive particles or, in terms of wave propagation, there is no well in the effective potential for these systems. To conclude, we show that one can mimic this instability in the laboratory using analogue acoustic black branes.

## 2. Rotating Kerr-like black branes

In this section we study in detail the black branes of the form (1.2). In higher dimensions there are several choices for rotation axes of the Myers-Perry solution (labeled $\mathrm{Kerr_d}$ in (1.2)) and there is a multitude of angular momentum parameters, each referring to a particular rotation axis [9]. We shall concentrate on the simplest case, for which there is only one angular momentum parameter, denoted by $a$.

### 2.1 Formalism

In Boyer-Lindquist-type coordinates the black branes we study in this section are described by

$$\begin{aligned} ds^2 = &-\frac{\Delta - a^2\sin^2\theta}{\Sigma}dt^2 - \frac{2a(r^2+a^2-\Delta)\sin^2\theta}{\Sigma}dt d\varphi + \\ &+\frac{(r^2+a^2)^2-\Delta a^2\sin^2\theta}{\Sigma}\sin^2\theta d\varphi^2 + \\ &+\frac{\Sigma}{\Delta}dr^2 + \Sigma d\theta^2 + r^2\cos^2\theta d\Omega_n^2 + dx^i dx_i\,, \end{aligned} \tag{2.1}$$

where

$$\Sigma = r^2 + a^2\cos^2\theta\,, \qquad \Delta = r^2 + a^2 - Mr^{1-n}\,, \tag{2.2}$$

and $d\Omega_n^2$ denotes the standard metric of the unit $n$-sphere ($n = \mathrm{d}-4$), the $x^i$ are the coordinates of the compact dimensions, and $i$ runs from 1 to $p$. This metric describes a rotating black brane in an asymptotically flat, vacuum space-time with mass and angular momentum proportional to $M$ and $Ma$, respectively. Hereafter, $M, a > 0$ are assumed.

The event horizon, homeomorphic to $S^{2+n}$, is located at $r = r_+$, such that $\Delta|_{r=r_+} = 0$. For $n = 0$, an event horizon exists only for $a < M/2$. When $n = 1$, an event horizon exists only when $a < \sqrt{M}$, and the event horizon shrinks to zero-area in the extreme limit $a \to \sqrt{M}$. On the other hand, when $n \geq 2$, $\Delta = 0$ has exactly one positive root for arbitrary $a > 0$. This means there is no bound on $a$, and thus there are no extreme Kerr black branes in higher dimensions.



JHEP07(2005)009

Consider now the evolution of a massless scalar field $\Psi$ in the background described by (2.1). The evolution is governed by the curved space Klein-Gordon equation

$$\frac{\partial}{\partial x^{\mu}}\left(\sqrt{-g}\, g^{\mu\nu}\frac{\partial}{\partial x^{\nu}}\Psi\right)=0\,, \tag{2.3}$$

where $g$ is the determinant of the metric. We can simplify considerably equation (2.3) if we separate the angular variables from the radial and time variables, as is done in four dimensions [10]. This separation was accomplished, for higher dimensions, in [11] for five dimensional Kerr holes and also in [12] for a general $4+n$-dimensional Kerr hole. Since we are considering only one angular momentum parameter, the separation is somewhat simplified, and we can follow [13]. In the end our results agree with the results in [11, 12] with only one angular momentum parameter in their equations.

We consider the ansatz $\phi = e^{-\mathrm{i}\omega t+\mathrm{i}m\varphi+\mathrm{i}\mu_i x^i}R(r)S(\theta)Y(\Omega)$, and substitute this form in (2.3), where $Y(\Omega)$ are hyperspherical harmonics on the $n$-sphere, with eigenvalues given by $-j(j+n-1)$ $(j=0,1,2,\cdots)$. Then we obtain the separated equations

$$\begin{aligned}\frac{1}{\sin\theta\cos^n\theta}\left(\frac{d}{d\theta}\sin\theta\cos^n\theta\frac{dS}{d\theta}\right)+\\ +\left[a^2(\omega^2-\mu^2)\cos^2\theta-m^2\csc^2\theta-j(j+n-1)\sec^2\theta+A\right]S=0\,,\end{aligned} \tag{2.4}$$

and

$$r^{-n}\frac{d}{dr}\left(r^n\Delta\frac{dR}{dr}\right)+\left\{\frac{\left[\omega(r^2+a^2)-ma\right]^2}{\Delta}-\frac{j(j+n-1)a^2}{r^2}-\lambda-\mu^2r^2\right\}R=0\,, \tag{2.5}$$

where $A$ is a constant of separation, $\lambda := A-2m\omega a+\omega^2a^2$, and $\mu^2=\sum\mu_i^2$. Interestingly, note the important point that Equations (2.4)-(2.5) are just those that describe the evolution of a massive scalar field, with mass $\mu$, in a d$-$dimensional Kerr geometry.

The equations (2.4) and (2.5) must be supplemented by appropriate boundary conditions, which are given by

$$R\sim\begin{cases}(r-r_+)^{-\mathrm{i}\sigma} & \text{as } r\to r_+\,,\\ r^{-(n+2)/2}\mathrm{e}^{\mathrm{i}\sqrt{\omega^2-\mu^2}r} & \text{as } r\to\infty\,,\end{cases} \tag{2.6}$$

with

$$\sigma\equiv\frac{\left[(r_+^2+a^2)\omega-ma\right]r_+}{(n-1)(r_+^2+a^2)+2r_+^2}\,. \tag{2.7}$$

In other words, the waves must be purely ingoing at the horizon and purely outgoing at the infinity. For assigned values of the rotational parameter $a$ and of the angular indices $l\,,j\,,m$ there is a discrete (and infinite) set of frequencies called quasinormal frequencies, QN frequencies or $\omega_{QN}$, satisfying the wave equation (2.5) with the boundary conditions just specified by eq. (2.6). Since the time-dependence of the mode is $e^{-\mathrm{i}\omega t}$, unstable modes will have frequencies with a *positive* imaginary part, and thus grow exponentially with time.

### 2.2 The physical nature of the instability

The equations presented in the previous section are amenable to numerical calculations (*infra*), but don't offer much physical insight into the physics. To gain some more intuition, and understand *why* we expected an instability to be triggered, we find it convenient to make instead the following change of variables, following Furuhashi and Nambu [8]:

$$R = r^{-n/2-1}\Psi\,, \tag{2.8}$$

in which case the wave equation (2.5) is transformed into

$$\frac{d^2\Psi}{dz_*^2} - V\Psi = 0\,. \tag{2.9}$$

Here, we have defined the modified tortoise coordinate $z_*$ as $\frac{dr}{dz_*} = \frac{\Delta}{r^2}$. (Note that the usual definition of the tortoise coordinate $r_*$ is $dr/dr_* = \Delta/(r^2+a^2)$).

The effective potential $V$ is equal to

$$\begin{aligned}-V = {}& \frac{1}{r^2}\left(-\lambda - a^2\mu^2 - \frac{n}{2} - \frac{n^2}{4} - 2am\omega + 2a^2\omega^2\right) + \\ &+\frac{a^2}{r^4}(a^2\omega^2 - 2am\omega - \frac{n^2}{2} - jn + m^2 - \lambda - j^2 + j + 2) + \\ &+\frac{a^4}{r^6}\left(2 + j - j^2 + \frac{n}{2} - nj - \frac{n^2}{4}\right) + \frac{\mu^2 M}{r^{n+1}} + \frac{M}{r^{n+3}}\left(\lambda - 1 - \frac{n}{2}\right) + \\ &+\frac{M^2}{r^{n+4}}\left(1 + n + \frac{n^2}{4}\right) + \frac{Ma^2}{r^{n+5}}\left(j^2 - j - 3 + jn + \frac{3n}{2}\right) + \omega^2 - \mu^2\,.\end{aligned} \tag{2.10}$$

Upon close inspection, this potential has two key ingredients which can trigger the instability: superradiant amplification of scattered waves and the existence of bound states. We shall briefly explore and describe these features in what follows.

#### 2.2.1 Superradiant scattering

In a scattering experiment (with $\omega > \mu$ so that plane waves at infinity are possible), equation (2.9) has the following asymptotic behavior:

$$\Psi_1 \sim \begin{cases} T(r-r_+)^{-\mathrm{i}\sigma} & \text{as } r \to r_+\,, \\ R\mathrm{e}^{\mathrm{i}\sqrt{\omega^2-\mu^2}r} + \mathrm{e}^{-\mathrm{i}\sqrt{\omega^2-\mu^2}r} & \text{as } r \to \infty\,. \end{cases} \tag{2.11}$$

where $\sigma$ was defined in the previous section, equation (2.7).

These boundary conditions correspond to an incident wave of unit amplitude from $+\infty$ giving rise to a reflected wave of amplitude $R$ going back to $+\infty$ and a transmitted wave of amplitude $T$ at $-\infty$ (as before, the boundary conditions we impose do not allow for waves emerging from the horizon). Since the potential is real, the complex conjugate of the solution $\Psi_1$ satisfying the boundary conditions (2.11) will satisfy the complex-conjugate boundary conditions:

$$\Psi_2 \sim \begin{cases} T^*(r-r_+)^{\mathrm{i}\sigma} & \text{as } r \to r_+\,, \\ R^*\mathrm{e}^{-\mathrm{i}\sqrt{\omega^2-\mu^2}r} + \mathrm{e}^{\mathrm{i}\sqrt{\omega^2-\mu^2}r} & \text{as } r \to \infty\,. \end{cases} \tag{2.12}$$

Now, these two solutions are linearly independent, and standard theory of ODE tells us that their wronskian is a constant (independent of $r$). If we evaluate the wronskian near the horizon, we get

$$W = -2\mathrm{i}\sigma A|T|^2 \tag{2.13}$$

where the constant $A$ is defined by

$$A = \frac{\Delta}{r^2(r - r_+)}\,, \qquad r \to r_+\,, \tag{2.14}$$

and is positive definite. Evaluating the wronskian at infinity we get

$$W = 2\mathrm{i}\sqrt{\omega^2 - \mu^2}(|R|^2 - 1)\,. \tag{2.15}$$

Equating the two we get

$$|R|^2 = 1 - \frac{\sigma A}{\sqrt{\omega^2 - \mu^2}}|T|^2\,. \tag{2.16}$$

Now, in general $|R|^2$ is less than unity, as is to be expected. However, for

$$\omega - \frac{ma}{r_+^2 + a^2} < 0\,, \tag{2.17}$$

we have that $\sigma$ is negative, and therefore in this regime (which will be referred to as the superradiant regime) $|R|^2 > 1$. This means that one gets back more than one threw in. Of course the excess energy comes from the hole's rotational energy, which therefore decreases. As a final remark, we notice that we have been assuming without loss of generality $\omega > 0$, and thus superradiance only exists for $m > 0$, which are modes co-rotating with the black hole.

### 2.2.2 The potential well

The effective potential in four dimensions, d = 4, as given by (2.10) is plotted in figure 1, for $a \sim 0.5$ (in units of $M$), $\mu = 0.7$ and $\omega = 0.6878$. As can be seen from figure 1 the potential has, in the four-dimensional situation, two extremum between the event horizon and spatial infinity. The local minimum creates a "well"-like structure, which will be so important to trigger the instability. The potential is asymptotic to $(\mu^2 - \omega^2)$ at spatial infinity. That a well must necessarily arise in four dimensions can be seen from the asymptotic nature of the potential. In fact, for $n = 0$ and for large $r$, the potential in (2.10) behaves as

$$V \sim \mu^2 - \omega^2 - \mu^2 M r^{-1}\,, \qquad r \to \infty\,, \qquad n = 0\,. \tag{2.18}$$

Thus, the derivative is $V' \sim \frac{\mu^2 M}{r^2}$, which is positive. Thus a well necessarily arises.

The instability can now be easily explained: the waves get "trapped" inside the potential well and amplified by superradiance. Thus, an exponential growth of any initial perturbation is inevitable, and therefore an instability arises. This simple picture is accurate enough that it will allow us to predict if and when an instability is triggered.

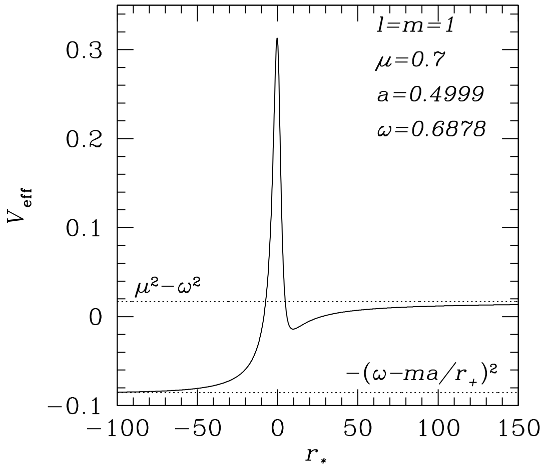


**Figure 1:** A typical form for the effective potential, here shown for $l = m = 1$ modes. We have set $M = 1$, so the rotation parameter $a$ varies between 0 (Schwarzschild limit) and 1/2 (extremal limit). Here we plot the effective potential for the near extreme situation, $a \sim 0.5$ and for $\mu = 0.7$ and $\omega = 0.6878$.

### 2.3 The numerical search technique

The problem we have to solve numerically is a simple boundary value problem of a second-order ordinary differential equation. However, this is not easy to solve with the usual techniques of direct integration, because of difficulties related to the absence of incoming radiation at the boundaries [14]. A standard technique to overcome the difficulties is the so-called Leaver's method [14], which we employ in this paper. In fact, this seems to be the first attempt at trying to find instabilities using this method, and it works well, as we shall see. In what follows, we shall describe the four dimensional ($n = 0$) case thoroughly, for concreteness. The method is easily adapted to any number of dimensions $n$, but the equations get much lengthier, so we refrain from presenting them here. We pick units such that $M = 1$. First, let us consider the radial equation. Following Leaver, the radial function $R$ can be expanded around the horizon as

$$R = (r - r_+)^{-i\sigma}(r - r_-)^{-1+i\sigma+i\mu^2(2\omega_1)^{-1}+i\omega_1}\mathrm{e}^{i\omega_1 r}\sum_{k=0}^{\infty} b_k \left(\frac{r - r_+}{r - r_-}\right)^k , \tag{2.19}$$

where $\sigma$ and $\omega_1$ are defined by

$$\sigma = \frac{(r_+^2 + a^2)\omega - ma}{a^2 + 3r_+^2}\, r_+ , \qquad \omega_1 = \sqrt{\omega^2 - \mu^2} . \tag{2.20}$$

Here, $b_0$ is taken to be $b_0 = 1$, and $r_+$ and $r_-$ are, respectively, the coordinate radius of the event and the Cauchy horizon of the Kerr black hole, given by $r_\pm = (1 \pm b)/2$, where $b = (1 - 4a^2)^{1/2}$. Note that the branch of $\sqrt{z}$ has been chosen such that $-\pi/2 < arg\sqrt{z} \leq \pi/2$. The expansion coefficients $b_k$ in equation (2.19) are determined via the five-term recurrence relation, given by

$$\alpha_0 b_1 + \beta_0 b_0 = 0 , \qquad \alpha_1 b_2 + \beta_1 b_1 + \gamma_1 b_0 = 0 , \qquad \alpha_2 b_3 + \beta_2 b_2 + \gamma_2 b_1 + \delta_2 b_0 = 0 ,$$



JHEP07(2005)009

$$\alpha_k b_{k+1} + \beta_k b_k + \gamma_k b_{k-1} + \delta_k b_{k-2} + \epsilon_k b_{k-3} = 0\,, \qquad k = 3, 4, 5, \ldots\,, \tag{2.21}$$

where

$$\begin{aligned} \alpha_k &= (1+k)(1+k+h_0)\,, \qquad \beta_k = -4k^2 + h_1 k + o_1\,, \qquad \gamma_k = 6k^2 + h_2 k + o_2\,, \\ \delta_k &= -4k^2 + h_3 k + o_3\,, \qquad \epsilon_k = k^2 + h_4 k + o_4\,. \end{aligned} \tag{2.22}$$

Here, the coefficients appearing in equation (2.22) are given by

$$\begin{aligned} h_0 &= -ib^{-1}\{-2am + \omega(1+b)\}\,, \\ h_1 &= -2 - 8iamb^{-1} + i\{4\omega b^{-1}(1+b) + \mu^2\omega_1^{-1} + 2\omega_1(1+b)\}\,, \\ h_2 &= -i(b\omega_1)^{-1}[6\omega_1(\omega - 2am) + 4b^2\omega_1^2 + 3b\{\mu^2 + 2\omega_1(\omega + \omega_1 - i)\}]\,, \\ h_3 &= 10 - 8iamb^{-1} + i\{4\omega(1+b^{-1}) + 3\mu^2\omega_1^{-1} + 2\omega_1(3+b)\}\,, \\ h_4 &= -i(b\omega_1)^{-1}[\omega_1(\omega - 2am) + b\{\mu^2 + \omega_1(\omega + 2\omega_1 - 4i)\}]\,, \end{aligned} \tag{2.23}$$

and

$$\begin{aligned} o_1 &= (4b\omega_1^2)^{-1}\big[b^3\omega_1^4 + 2(2am - \omega)\{-2\omega^2(i + \omega + \omega_1) + \mu^2(2i + 2\omega + \omega_1)\} - \\ &\qquad - 2b^2\omega_1^2\{\mu^2 - 2(\omega^2 + i\omega_1(i + \omega))\} + \\ &\qquad + b\{\mu^4 + \mu^2(4 + 4A_{lm} - 4i\omega - 8\omega^2 - 2i\omega_1 + 8am\omega_1 - 6\omega\omega_1) \\ &\qquad + \omega^2(-4 - 4A_{lm} + 4i\omega + 7\omega^2 + 4i\omega_1 - 8am\omega_1 + 8\omega\omega_1)\}\big]\,, \\ o_2 &= (4b\omega_1^2)^{-1}\big[-2b^3\omega_1^4 - 4b^2\{\mu^4 - \mu^2(3\omega^2 + 2i\omega_1 + 2\omega\omega_1) + \\ &\qquad\qquad + 2(\omega^4 + i\omega^2\omega_1 + \omega^3\omega_1 - 2i\omega_1^3)\} - \\ &\qquad - 6(2am - \omega)\{\mu^2(2i + 2\omega + \omega_1) - 2(\omega^3 - 2i\omega_1^2 + \omega^2(i + \omega_1))\} + \\ &\qquad + b\{-3\mu^4 - 2\mu^2(6 + 4A_{lm} - 6i\omega - 10\omega^2 - 10i\omega_1 + 8am\omega_1 - 7\omega\omega_1) + \\ &\qquad\quad + 2(-9\omega^4 + 12i\omega\omega_1^2 + 12i\omega_1^3 - 2\omega^3(3i + 5\omega_1) + \\ &\qquad\qquad + \omega^2(6 + 4A_{lm} - 8i\omega_1 + 8am\omega_1))\}\big]\,, \\ o_3 &= (4b\omega_1^2)^{-1}[b^3\omega_1^4 + b\{3\mu^4 + 15\omega^4 - 32i\omega\omega_1^2 - 16\omega_1^2(1 + 3i\omega_1) + 4\omega^3(3i + 4\omega_1) - \\ &\qquad\qquad - 4\omega^2(3 + A_{lm} - 5i\omega_1 + 2am\omega_1) + \\ &\qquad\qquad + 2\mu^2(6 + 2A_{lm} - 6i\omega - 8\omega^2 - 17i\omega_1 + 4am\omega_1 - 5\omega\omega_1)\} + \\ &\qquad + 2b^2\{\mu^4 - \mu^2(3\omega^2 + 2i\omega_1 + 2\omega\omega_1) + 2(\omega^4 + i\omega^2\omega_1 + \omega^3\omega_1 - 4i\omega_1^3)\} + \\ &\qquad + 2(2am - \omega)\{3\mu^2(2i + 2\omega + \omega_1) - 2(3\omega^3 - 8i\omega_1^2 + 3\omega^2(i + \omega_1))\}\big]\,, \\ o_4 &= (4b\omega_1^2)^{-1}\big[-2(2am - \omega)\{\mu^2(2i + 2\omega + \omega_1) - 2(\omega^3 - 3i\omega_1^2 + \omega^2(i + \omega_1))\} + \\ &\qquad + b\{-\mu^4 - 4(\omega^4 + \omega^2(-1 + 2i\omega_1) - 3i\omega\omega_1^2 - 3\omega_1^2(1 + 2i\omega_1) + \\ &\qquad\quad + \omega^3(i + \omega_1)) + 2\mu^2(-2 + 2\omega^2 + 8i\omega_1 + \omega(2i + \omega_1))\}\big]\,, \end{aligned} \tag{2.24}$$

Using gaussian elimination twice, one can reduce the five-term recurrence relations (2.21) to three-term recurrence relations, which can be written as

$$\alpha'_0 b_1 + \beta'_0 b_0 = 0\,, \qquad \alpha'_k b_{k+1} + \beta'_k b_k + \gamma'_k b_{k-1}\,, \qquad k = 1, 2, \ldots \tag{2.25}$$

Since the gaussian elimination is straightforward, we do not show an explicit procedure for the gaussian elimination (see, e.g., [15]). An eigenfunction satisfying the quasinormal mode boundary conditions behaves at the event horizon and infinity as

$$\Psi \sim \begin{cases} (r-r_+)^{-i\sigma} & \text{as } r \to r_+ \,, \\ r^{-1+i\mu^2(2\omega_1)^{-1}+i\omega_1} \mathrm{e}^{i\omega_1 r} & \text{as } r \to \infty \,. \end{cases} \tag{2.26}$$

Therefore, one can see that the expanded wave function (2.19) satisfies the quasinormal mode boundary conditions if the expansion in (2.19) converges at spatial infinity. This convergence condition for the expansion (2.19), namely the quasinormal mode conditions, can be written in terms of the continued fraction as [16, 14]

$$\beta'_0 - \frac{\alpha'_0\gamma'_1}{\beta'_1-}\frac{\alpha'_1\gamma'_2}{\beta'_2-}\frac{\alpha'_2\gamma'_3}{\beta'_3-}\cdots \equiv \beta'_0 - \cfrac{\alpha'_0\gamma'_1}{\beta'_1 - \cfrac{\alpha'_1\gamma'_2}{\beta'_2 - \cfrac{\alpha'_2\gamma'_3}{\beta'_3 - \cdots}}} = 0\,, \tag{2.27}$$

where the first equality is a notational definition commonly used in the literature for infinite continued fractions. Here, we shall adopt this convention.

Next, we turn ourself to the angular equation. In order to determine the separation constant $A_{lm}$, a similar technique to that used for the radial equation can be applied. Imposing regularity on the symmetry axis, we can expand the angular function as

$$S = \mathrm{e}^{a\omega_1 u}(1-u^2)^{\frac{|m|}{2}} \sum_{k=0}^{\infty} d_k (1+u)^k \,, \tag{2.28}$$

where $u = \cos\theta$, and $d_0 = 1$. The expansion coefficients $d_k$ in equation (2.28) are determined via the three-term recurrence relation, given by

$$\tilde{\alpha}_0 d_1 + \tilde{\beta}_0 d_0 = 0\,, \qquad \tilde{\alpha}_k d_{k+1} + \tilde{\beta}_k d_k + \tilde{\gamma}_k d_{k-1} = 0\,, \qquad k = 1, 2, 3, \dots\,, \tag{2.29}$$

where

$$\begin{aligned} \tilde{\alpha}_k &= -2(1+k)(k+|m|+1)\,, \\ \tilde{\beta}_k &= k(k-1) + 2k(|m|+1-2a\omega_1) - (2a\omega_1 - |m|)(|m|+1) - (a^2\omega_1^2 + A_{lm})\,, \\ \tilde{\gamma}_k &= 2a\omega_1(k+|m|)\,. \end{aligned} \tag{2.30}$$

Note that in the four dimensional case, we have to set $j = 0$ in equations (2.5) and (2.6). If the expansion in equation (2.28) converges for $-1 \le u \le 1$, the angular function satisfies the regularity conditions at $u = \pm 1$. This condition is equivalent to the continued fraction equation, given by [16, 14]

$$\tilde{\beta}_0 - \frac{\tilde{\alpha}_0\tilde{\gamma}_1}{\tilde{\beta}_1-}\frac{\tilde{\alpha}_1\tilde{\gamma}_2}{\tilde{\beta}_2-}\frac{\tilde{\alpha}_2\tilde{\gamma}_3}{\tilde{\beta}_3-}\cdots = 0\,, \tag{2.31}$$

Now that we have two continued fraction equations of the frequency $\omega$ and the separation constant $A_{lm}$ (2.27) and (2.31), we can obtain the frequency $\omega$ and the separation constant $A_{lm}$ solving equations (2.27) and (2.31) simultaneously. These coupled algebraic equations (2.27) and (2.31) can be solved numerically (see, e.g., [17, 18]).



JHEP07(2005)009

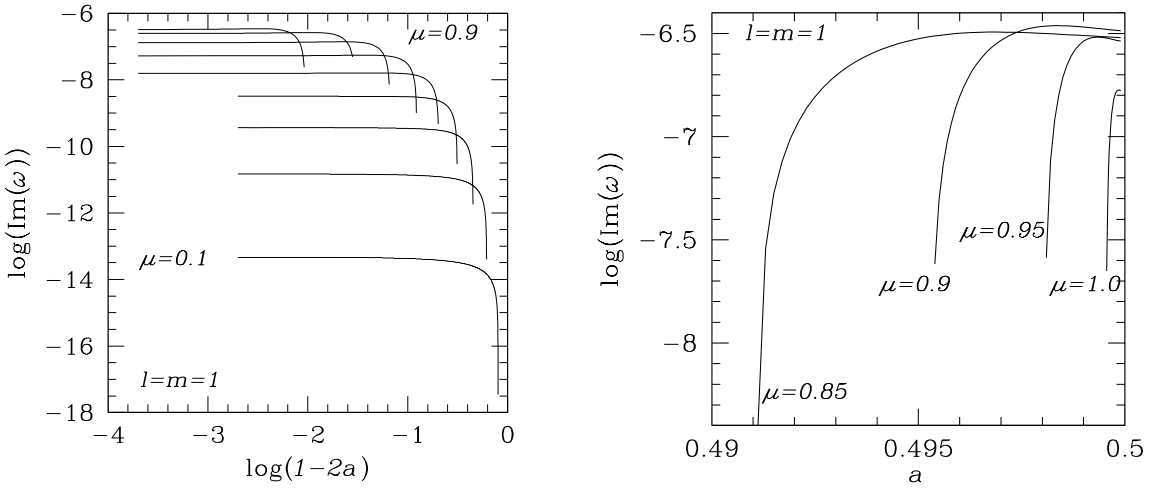


**Figure 2:** Details for the instability in the four dimensional case. We have set $M = 1$, so the rotation parameter $a$ varies between 0 (Schwarzschild limit) and 1/2 (extremal limit). In the left panel we plot the imaginary part of the unstable modes as a function of $a$ for nine values of $\mu$, and for $l = m = 1$. The same quantities are plotted in the right panel, but now we focus on the maximum instability region, for values of $\mu$ near unity. The instability is stronger for larger values of $a$ and for $\mu \sim 1$. In fact, our results suggest that the imaginary part of the unstable modes attains its maximum value, $10^{-6} \times \mathrm{Re}[\omega]$ for $\mu = 0.9$ and $a = 0.497$. Notice finally that as one decreases $a$ (going right on the $x$ axis in the left panel), there is a critical $a$ below which there is no instability. Although there are an infinity of unstable modes, we only show here the most unstable one.

### 2.4 The instability for the $\mathrm{d} = 4$ case

Some numerical results for $\mathrm{d} = 4$ were given by Furuhashi and Nambu [8] and also by Strafuss and Khanna [8], in the context of massive field instability of the Kerr metric which as we saw, translate immediately to our situation. Nevertheless, we have performed an independent extensive numerical search, which allow us to have a more complete picture and understanding of the situation. Our numerical results were obtained using the technique just described *supra*, and are summarized in figures 2–3. There is more than one frequency with a positive imaginary part, corresponding to unstable modes. We only show the most relevant one which is the one having a larger imaginary part, and therefore corresponds to the most unstable mode.

In figure 2 we plot the imaginary part of the (unstable) mode as a function of $a$ for several values of $\mu$ and for $l = m = 1$. The instability timescale is given by $\tau \sim \frac{1}{\mathrm{Im}[\omega]}$. We can see that:

(i) The instability gets stronger (the typical timescale decreases) as the rotation $a$ increases. This is expected, since we know that the superradiant amplification gets stronger as $a$ increases [6, 19].

(ii) The instability also gets stronger as $\mu$ increases. This has a very simple explanation: the depth of the potential well in figure 1 is larger for larger values of $\mu$, and therefore

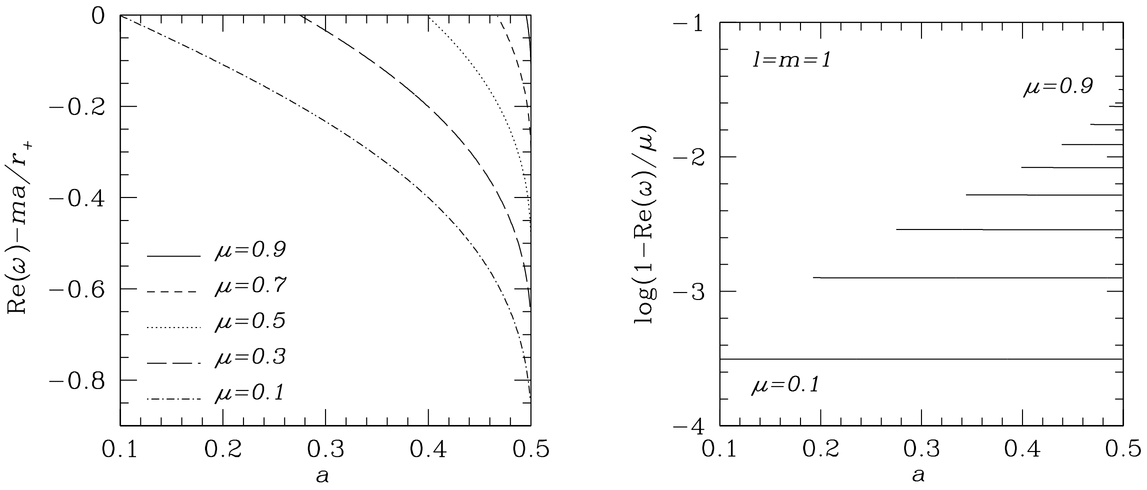


**Figure 3:** More details of the instability in the four dimensional case. Here we plot the superradiant factor $\mathrm{Re}[\omega]-\frac{ma}{a^2+r_+^2}$ as a function of $a$ for $l=m=1$ and for several values of $\mu$. Again, we have set $M=1$ and so the superradiant factor is, in four dimensions, $\mathrm{Re}[\omega]-\frac{ma}{r_+}$. the instability disappears for $a$ below a certain critical point, which is given by setting the superradiant factor to zero. On the right panel we make the same plot but on a logarithmic scale, for better visualization. Notice that the superradiant factor is negative, as it should for the instability to be triggered.

the waves get more efficiently trapped. Our results suggest that the imaginary part of the unstable modes attains its maximum value, $10^{-6}\times \mathrm{Re}[\omega]$ for $l=m=1$, $\mu=0.9$ and $a=0.497$.

(iii) For a fixed $\mu$ and as one decreases $a$ the unstable modes disappear below a certain critical value of $a$. This is because the superradiance condition $\mathrm{Re}[\omega]-\frac{ma}{a^2+r_+^2}<0$ is not satisfied for very low rotation parameter $a$. This is best seen in figure 3.

In figure 3 we plot the real part of the (unstable) mode as a function of $a$ for several values of $\mu$ and for $l=m=1$. Two important features are the following:

(i) As shown in both plots of figure 3, the superradiant factor $\mathrm{Re}[\omega]-\frac{ma}{a^2+r_+^2}$ is negative, and one is therefore in the superradiant regime. Thus, this is indeed a superradiant instability.

(ii) The instability occurs only for $\omega<\mu$. Otherwise, the waves would not be trapped in the potential well, but they would rather escape to infinity, and the perturbation would be damped.

Detweiler [8] finds (in four dimensions), in the limit of small $\mu$, that the characteristic frequencies of the unstable modes are, in our units,

$$\omega\sim\mu+\mathrm{i}\mu\frac{a}{M}\frac{(\mu M)^8}{3072}\,. \tag{2.32}$$

Our numerical results fit this prediction very well. For near-extremal black holes, and $\mu\sim 0.1$ Detweiler's formula (2.32) predicts $\omega\sim 0.1+10^{-13}\mathrm{i}$, which checks very well with our numerics (see figure 2 and 3).

Although of no direct interest for this work, we found also stable modes. Our results for stable modes will be published elsewhere [22], and compared with the existing analytical ones [23].

### 2.5 No instability for higher dimensional rotating Kerr-like black branes

We have also performed a numerical search for the instability in the d $= 5\,,6\,,7$ case. We found no trace of unstable modes, and we justify this in a rigorous analysis presented in appendix A. We now turn to explain why higher dimensional Kerr-like branes should be stable against this particular mechanism.

We saw that the instability arises because of superradiantly amplified trapped modes, in the potential well. But does a well exist for general d? It doesn't, and to understand this, we have to look at the asymptotic behavior of the effective potential (2.10). If the derivative of this potential is positive near spatial infinity, we are guaranteed to have a well, and therefore an instability. If the derivative is negative, the modes should all be stable. Near infinity, the dominant terms in the effective potential (2.10) are

$$V' \sim -\frac{2}{r^3}\left(A_{lm}+a^2\mu^2+\frac{n}{2}+\frac{n^2}{4}-a^2\omega^2\right)+(n+1)\mu^2 M r^{-2-n}\,, \tag{2.33}$$

where we have already substituted for the separation constant $\lambda = A_{lm} - 2am\omega + a^2\omega^2$. It is immediately apparent that the four dimensional case is a special one: if $n = 0$, the dominant term in the derivative is $(n+1)\mu^2 M r^{-2-n}$, which is positive and we therefore are guaranteed to have a bound state. Thus, this case should be unstable, and it is, as we just described in the previous subsection.

When $n > 0$ the other terms dominate. In fact, for $n > 1$ they are positive. For $n > 1$ the dominant terms are

$$V' \sim -\frac{2}{r^3}\left(A_{lm}+a^2\mu^2+\frac{n}{2}+\frac{n^2}{4}-a^2\omega^2\right). \tag{2.34}$$

Since $\omega < \mu$, this is negative (the separation constant $A_{lm}$ can be shown to be positive). Thus, for d $> 5$ there is no potential well, no bound states and therefore no instability, even though there is still superradiance. The situation for $n = 1$ is not as clear, because there is the extra term $(n+1)\mu^2 M r^{-2-n}$. In principle it should be possible to have, for certain very specific parameters, a potential well. But to do that, one would have to require that $\mu$ be very large, and this makes it very hard to study the problem numerically (the imaginary part is expected to be extremely small in this regime, as shown by Zouros and Eardley [8], and this prevents any numerical treatment).

There is another, perhaps more physical, explanation of the fact that higher dimensional rotating black branes should be stable. We know that the a massless field propagating in the background of these rotating black branes is equivalent to a massive field propagating in the background of a Myers-Perry black hole. Imagine now a wavepacket of the massive field in a distant circular orbit. In the four-dimensional situation, the gravitational force binds the field and keeps it from escaping or radiating away to infinity. But at the event horizon some of the field goes down the black hole, and if the frequency of the field is in the superradiant region then the field is amplified. Hence the field is amplified at the event horizon while being bound away from infinity. We should thus have an instability, as we do. However, for d $> 4$, there are no stable orbits,[1] and thus the field escapes to infinity, no instability is triggered. This complements the previous view point. Escaping to infinity is equivalent to not having a potential well to bound the field.

## 3. Acoustic black branes

In 1981 Unruh [24] introduced the notion of "dumb holes", which is an example of analogue black holes. While not carrying information about Einstein's equations, the analogue black holes devised by Unruh do have a very important feature that defines black holes: the existence of an event horizon. The basic idea behind these analogue acoustic black holes is very simple: consider a fluid moving with a space-dependent velocity, for example water flowing throw a variable-section tube. Suppose the water flows in the direction where the tube gets narrower. Then the fluid velocity increases downstream, and there will be a point where the fluid velocity exceeds the local sound velocity, in a certain frame. At this point, in that frame, we get the equivalent of an apparent horizon for sound waves. In fact, no (sonic) information generated downstream of this point can ever reach upstream (for the velocity of any perturbation is always directed downstream, as a simple velocity addition shows). This is the acoustic analogue of a black hole, or a *dumb hole*. We refer the reader to [25] for a review of these objects.

### 3.1 The wave equation for a general space-dependent density

We can also model acoustic black branes easily, and we can thus look for the instability dealt with here in the laboratory. For simplicity, let us consider the following black brane. First build a 2+1 dimensional acoustic black hole [25], modelling a draining bathtub. Consider a fluid having (background) density $\rho(x)$. Assume the fluid to be locally irrotational (vorticity free), barotropic and inviscid. From the equation of continuity, the radial component of the fluid velocity satisfies $\rho v^r \sim 1/r$. Irrotationality implies that the tangential component of the velocity satisfies $v^\theta \sim 1/r$. We shall keep both $\rho$ and the sound velocity $c$ as position-dependent quantities, thus generalizing the treatment in [25, 26]. We then have

$$v^r = \frac{A}{\rho r}\,, \qquad v^\theta = \frac{B}{r}\,, \tag{3.1}$$

where $A\,,\,B$ are constants. The acoustic metric describing the propagation of sound waves in this "draining bathtub" fluid flow is [25]:

$$ds^2 = -\left(c^2 - \frac{A^2/\rho^2 + B^2}{r^2}\right)dt^2 + \frac{2A}{\rho r}drdt - 2Bd\phi dt + dr^2 + r^2 d\phi^2\,. \tag{3.2}$$

[1] Tangherlini [20], who discovered the higher dimensional Schwarzschild solution, also proved there are no stable circular geodesics in these spacetimes for d $> 4$. There is, to our knowledge, no proof of this statement for higher dimensional Kerr black holes, but it was shown in [21] that the five-dimensional Kerr solution doesn't have stable circular geodesics, along the equatorial plane. It seems very likely that stable orbits do not exist in the general case.



JHEP07(2005)009

It is however better to work with a more transparent metric. Some physical properties of this draining bathtub metric are more apparent if we cast the metric in a Kerr-like form performing the following coordinate transformation (see [26, 27]):

$$dt \to d\tilde{t} = dt - \frac{Ar/\rho}{r^2c^2 - A^2/\rho^2}dr \tag{3.3}$$

$$d\phi \to d\tilde{\phi} = d\phi - \frac{BA/\rho}{r(r^2c^2 - A^2/\rho^2)}dr\,, \tag{3.4}$$

Then the effective metric takes the form

$$ds^2 = -\left(1 - \frac{A^2/\rho^2 + B^2}{c^2r^2}\right)c^2d\tilde{t}^2 + \left(1 - \frac{A^2}{\rho^2c^2r^2}\right)^{-1}dr^2 - 2Bd\tilde{\phi}d\tilde{t} + r^2d\tilde{\phi}^2\,. \tag{3.5}$$

As explained in [26], this metric and the Kerr metric differ in an important aspect, in that whereas the rotation for the Kerr black hole is bounded from above, here it is not, at least in principle. Thus, $B$ could be as large as desired.

Now, we are free to add an extra dimension $z$ to this effective geometry, as explained by Visser [25], resulting in the following black brane geometry

$$ds^2 = -\left(1 - \frac{A^2/\rho^2 + B^2}{c^2r^2}\right)c^2d\tilde{t}^2 + \left(1 - \frac{A^2}{\rho^2c^2r^2}\right)^{-1}dr^2 - 2Bd\tilde{\phi}d\tilde{t} + r^2d\tilde{\phi}^2 + dz^2\,. \tag{3.6}$$

The propagation of a sound wave in a barotropic inviscid fluid with irrotational flow, which is assumed to be the case, is described by the Klein-Gordon equation $\nabla_\mu\nabla^\mu\Phi = 0$ for a massless field $\Psi$ in a lorentzian acoustic geometry. Separating variables by the substitution

$$\Phi(\tilde{t}, r, \tilde{\phi}) = \sqrt{r}\Psi(r)e^{i(\mu z + m\tilde{\phi} - \omega\tilde{t})}\,, \tag{3.7}$$

implies that $\Psi(r)$ obeys the wave equation

$$\frac{d^2\Psi}{dr_*^2} + \left((\omega - \frac{Bm}{r^2})^2 - V\right)\Psi = 0\,. \tag{3.8}$$

Here

$$V = f\left(\mu^2c + \frac{4m^2c - c}{4r^2} + \frac{5A^2}{4cr^4\rho^2} + \frac{c'}{2r} + \frac{A^2}{2cr^3\rho^2}(\frac{c'}{c} + \frac{2\rho'}{\rho})\right)\,, \tag{3.9}$$

and the tortoise coordinate $r_*$ is defined as

$$\frac{dr}{dr_*} = c(1 - \frac{A^2}{c^2\rho^2r^2}) \equiv f\,. \tag{3.10}$$

Notice that for constant $\rho$, $c$ one recovers the equations in [26, 27], as one should. Now, it is quite easy to present an example of background flow for which the instability is triggered: take for instance a flow for which $\rho$ is almost constant at infinity (almost means that it asymptotes to a constant value more rapidly than the sound velocity). Assume also that, near infinity, $c = c_1 + \frac{c_2}{r}$. Then, we get that near infinity the effective potential behaves as

$$\frac{2c_1c_2k^2}{r}\,. \tag{3.11}$$

For this to have a positive derivative, one requires $c_2 < 0$ ($c_1$ must be positive, as it is the asymptotic value of the sound velocity). We thus have one example of flow for which the instability is active. There are many others, of course, and there are also instances for which the system is stable. But the important point here, is that we *can* build this effective geometry in the lab, and thus observe this instability.

## 4. The endpoint of the instability

We have shown that many rotating black objects are unstable against the instability displayed here. We have also shown that, for a fixed mass term $\mu$, the instability disappears for a rotation parameter $a$ below a certain value, for which the superradiant factor $\mathrm{Re}[\omega]-\frac{ma}{a^2+r_+^2}$ is zero. Now, as the unstable mode grows, rotational energy is being extracted from the black brane, and thus its rotation decreases (the same phenomenon happens for the black hole bomb [6]). This means that eventually the instability stops growing, when the rotation is in the critical point, for which the superradiant factor is zero. It looks very tempting and reasonable to assume that the system will settle down to a low-rotation black brane plus some radiation around it. Eventually, all this radiation will escape to infinity. The total angular momentum of the system is conserved, so this radiation carries the extra angular momentum. This is also clear from the fact that only co-rotating modes are unstable. This is one possibility. But bearing in mind that these are bound modes, it seems plausible that one other thing could happen, before the radiation escapes to infinity: since we are dealing with higher dimensional objects, the end product could be an object with two or more components for the angular momentum, that is to say, there could be a transfer of angular momentum from one dimension to the other.

## 5. Conclusions

We have shown that there is a large class of extended rotating black objects which are unstable against *massless* field perturbations. The instability is caused by superradiant amplification of waves trapped inside the potential well, or from a different view-point, it is caused by superradiant amplification of wave packets bound by the gravitational force. This mechanism is very similar to other superradiant mechanisms in the presence of black holes [5, 6, 8], or other rotating objects such as stars [28]. The important point here is that the extra dimensions work as an effective mass for any massless field. Thus, the evolution of a massless scalar field in, for example, the black brane (1.2) is equivalent to the evolution of a massive field in the background of a Myers-Perry rotating black hole. In four dimensions, the black hole displays superradiance and has bound states due to the mass term, thus the geometry is unstable. In higher dimensions, the spacetimes dealt with here have no stable circular geodesics (the mass term does not give rise to a potential well in the wave description) and therefore these spacetimes are stable. This simple reasoning implies that general four dimensional extended rotating black objects (more general than the one described by (1.1)) will be unstable. It also seems to imply that general higher dimensional rotating black objects are stable. Moreover, following Zel'dovich [4], it is



JHEP07(2005)009

known that not only the Kerr geometry, but any rotating absorbing body for that matter displays superradiance. Thus, this instability appears also in analogue black hole models, as we have shown.

Here, we have derived the instability timescale for a scalar field, and not for geometry (metric) perturbations, since Teukolsky's formalism for higher dimensional rotating objects is still not available. Still, the argument presented above makes it clear that the instability should be present for metric perturbations as well. Indeed, the presence of the potential well, in four dimensions, is due only to the mass term, and not to the geometry properties themselves, and since metric modes also scatter superradiantly [19] then everything we discussed here translates immediately to metric perturbations. We also expect that the instability will be stronger for metric modes, because of the following simple reasoning. Superradiance is responsible for this instability, and thus the larger the superradiant effects, the stronger the instability. Now, we know that in the four dimensional Kerr geometry scalar fields have a maximum superradiant amplification factor of about 2%, whereas gravitational modes have maximum superradiant amplification factor of about 138% [19]. Thus, we expect the instability timescale to be almost two orders of magnitude smaller for gravitational modes, which means that the instability is two orders of magnitude more effective for metric modes. For general black branes, the Gregory-Laflamme instability seems to be stronger than the one displayed here, but it is known that certain extremal solutions should not exhibit the Gregory-Laflamme instability [29], whereas the instability dealt with here should go all the way to extremality. So eventually it takes over the Gregory-Laflamme instability. Moreover, recent studies [30] seem to indicate that black strings in a Randall-Sundrum inspired 2-brane model do not exhibit the Gregory-Laflamme instability, but they should be unstable against this mechanism.

It seems plausible to assume that the instability will keep growing until the energy and angular momentum content of the field approaches that of the black brane, when back-reaction effects become important. The rotating brane will then begin to spin down, and gravitational and scalar radiation goes off to infinity carrying energy and angular momentum. The system will probably be asymptotic to a static, or very slowly rotating, final state consisting of a non-rotating black p-brane and some outgoing radiation at infinity. The end product could also be an object with two or more components for the angular momentum, that is to say, there could be a transfer of angular momentum from one dimension to the other.

## Acknowledgments

We would like to thank Jim Meyer for a critical reading of the manuscript. V. C. acknowledges financial support from Fundação para a Ciência e Tecnologia (FCT) - Portugal through grant SFRH/BPD/2004. S.Y. is supported by the Grant-in-Aid for the 21st Century COE "Holistic Research and Education Center for Physics of Self-organization Systems" from the ministry of Education, Science, Sports, Technology, and Culture of Japan.

## A. Factorized potential analysis

We now present a full description of our search for bound states in general $(4+n)$-dimensions. We conclude that no unstable bound states exist for $n \geq 5$. The massive scalar field equation in 4+n dimensional spacetime is given by

$$\Delta r^{-n} \frac{d}{dr}\left(\Delta r^n \frac{dR}{dr}\right) + V_0 R = 0\,, \tag{A.1}$$

where $V_0$ is the effective potential, given by

$$V_0 = \{\omega(r^2+a^2) - am\}^2 - \Delta\left\{\mu^2 r^2 + A_{lm} - 2m\omega a + \omega^2 a^2 + \frac{j(j+n-1)a^2}{r^2}\right\}. \tag{A.2}$$

For simplicity, let us assume $A_{lm}$ to be $A_{lm} = l(l+1)$. Note that this assumption is only valid in the limit of $a^2(\omega^2 - \mu^2) \to 0$. Introducing a new variable $r_*$ and a normalized function $\Phi$, defined as

$$dr_* = \frac{r^2+a^2}{\Delta}\,dr\,, \qquad R = \{(r^2+a^2)r^n\}^{-\frac{1}{2}}\Phi\,, \tag{A.3}$$

we can reduce equation (A.2) to

$$\frac{d^2\Phi}{dr_*^2} + V\Phi = 0\,, \tag{A.4}$$

where

$$V = \frac{V_0}{(r^2+a^2)^2} - G^2 - \frac{dG}{dr_*}\,, \qquad G = \frac{d}{dr_*}\log[(r^2+a^2)r^n]^{\frac{1}{2}}\,. \tag{A.5}$$

Since $V$ is, due to the simplified $A_{lm}$, a quadratic function of $\omega$, it can be factorized as

$$V = \alpha(\omega - V_+)(\omega - V_-)\,, \tag{A.6}$$

where $V_+ \geq V_-$ and $\alpha$ is a positive function, given by

$$\begin{aligned}\alpha &= \frac{(r^2+a^2)^2 - \Delta a^2}{(r^2+a^2)^2} \\ &= \frac{(r^2+a^2)^2 - a^2(r^2+a^2-r^{1-n})}{(r^2+a^2)^2} \\ &= \frac{(r^2+a^2)r^2 + a^2 r^{1-n}}{(r^2+a^2)^2} > 0\,.\end{aligned} \tag{A.7}$$

Note that $\alpha$ also satisfies

$$\lim_{r\to r_+}\alpha = \lim_{r\to\infty}\alpha = 1\,. \tag{A.8}$$

The factorized potentials $V_\pm$ have the following properties:

$$\lim_{r\to r_+} V_\pm = \frac{ma}{r_+^2+a^2} = m\Omega\,, \qquad \lim_{r\to\infty} V_\pm = \pm\mu\,, \tag{A.9}$$

where $\Omega$ is the rotation frequency of the black hole at the horizon. Note that $V_+ = V_-$ is satisfied at the horizon.

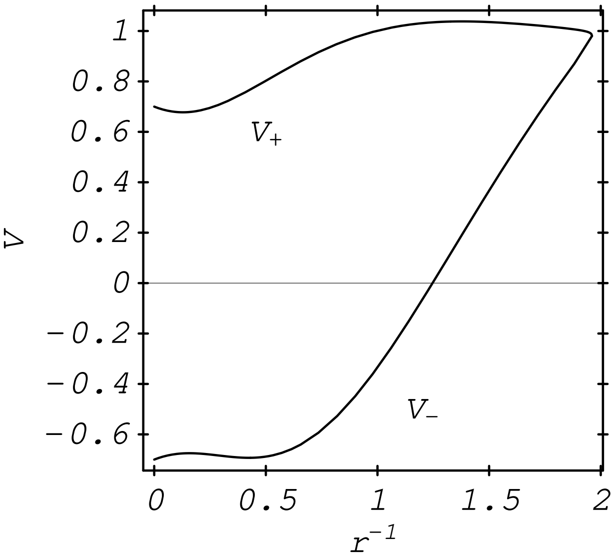


**Figure 4:** The factorized potentials $V_\pm$ as a function of $r^{-1}$. The potentials are characterized by $n = 0$, $l = m = 1$, $j = 0$, $\mu = 0.7$, and $a = 0.4999$.

The factorized potentials are quite useful to see how a solution behaves when the frequency $\omega$ is given. First, let us consider the four dimensional case, i.e. the n=0 case. Taking the case of $l = m = 1$, $j = 0$, $\mu = 0.7$, and $a = 0.4999$ as an example, we plot the typical behavior of the factorized potentials for the four dimensional case in figure 4. Since $\alpha$ is positive definite, the field $\Phi$ has propagative (evanescent) character when $\omega > V_+$ or $\omega < V_-$ ($V_- < \omega < V_+$) because $\Phi^{-1}d^2\Phi/dr_*^2 < 0$ ($\Phi^{-1}d^2\Phi/dr_*^2 > 0$) there. In other words, the region where $\omega > V_+$ or $\omega < V_-$ ($V_- < \omega < V_+$) is a classically allowed (forbidden) one. By a factorized potential diagram, we can then see where is the propagative or evanescent zone once the frequency $\omega$ is given.

Next, let us consider bound states for our problem. To have a bound state, we need a propagative zone between evanescent zones. That is to say, unless $V_+$ ($V_-$) does have a local minimum (maximum), there are no bound state in the potential. We can therefore expect from the behavior of $dV_\pm/dr$ whether bound states are possible or not. In figure 5, we display the $dV_+/dr = 0$ curve on the $r^{-1}$ — $\mu$ plan for the case of $l = m = 1$, $j = 0$, and $a = 0.4999$. From the figure, we can confirm that $V_+$ as a function of $r$ have two extremes for $0 \leq \mu < 1.321$. From figure 4, we can indeed see that $V_+$, in which $\mu = 0.7$, has a local minimum near $r^{-1} = 0.15$ and that there is a potential bound state if we take $\omega \sim 0.6878$, which is a correct eigenfrequency of the bound states. Another important thing is that $\omega \sim 0.6878$ is below $m\Omega$, which can be easily seen from the factorized potential diagrams. This means that this bound state is an unstable mode because it satisfies the condition of the superradiant instability.

Now, let us move on to higher dimensions, taking $n = 1$ to be specific. Consider the case of $l = m = 1$ and $j = 0$ as an example. We are interested in finding out whether or not there can be bound states in the five dimensional case. In order to see the distribution of extremes of $V_+$, which give us a criterion for nonexistence of the bound states, a curve

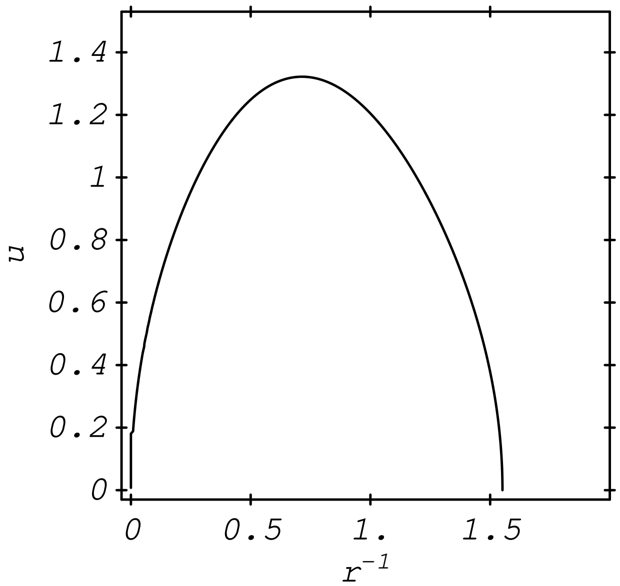


**Figure 5:** The curve of $dV_+/dr(r^{-1}, \mu) = 0$ for the parameter $n = 0$, $l = m = 1$, $j = 0$, and $a = 0.4999$.

of $dV_+/dr(r, \mu) = 0$ on the $r^{-1}$ — $\mu$ plan is sketched in figure 6, where the black hole characterized by $a = 0.9$ is taken. In the figure, it is found that if the mass $\mu$ satisfies $1.658 \leq \mu < 1.784$, $dV_+/dr$ as a function of $r$ has two zeros; one corresponds to a local maximum of $V_+$ and the other a local minimum of $V_+$. It should be emphasized that contrary to the four dimensional case, there is a critical mass below which no potential bound state exists. Therefore, there is the possibility that a bound state exists in the five dimensional case. A distribution of $V_+$ for the case of $\mu = 1.75$ is shown in figure 7. We can conclude from the figure that all the frequencies for potential bound states are always above $m\Omega$. Therefore, those potential bound states must not be unstable against the superradiance instability even if they exist. For other sets of the parameters, we have found similar behavior of the factorized potential. This means that in the five dimensional case, there might be bound states but all the potential bound stats are stable. This analysis is consistent with our numerical studies, in which we have not found any unstable modes.

For general $n > 5$ the trend is the same, there are no unstable bound states.

## References


[1] D. Marolf and B.C. Palmer, *Gyrating strings: a new instability of black strings?*, *Phys. Rev.* **D 70** (2004) 084045 [hep-th/0404139].

[2] V. Cardoso and J.P.S. Lemos, *New instability for rotating black branes and strings*, hep-th/0412078.

[3] T. Regge and J.A. Wheeler, *Stability of a schwarzschild singularity*, *Phys. Rev.* **108** (1957) 1063.

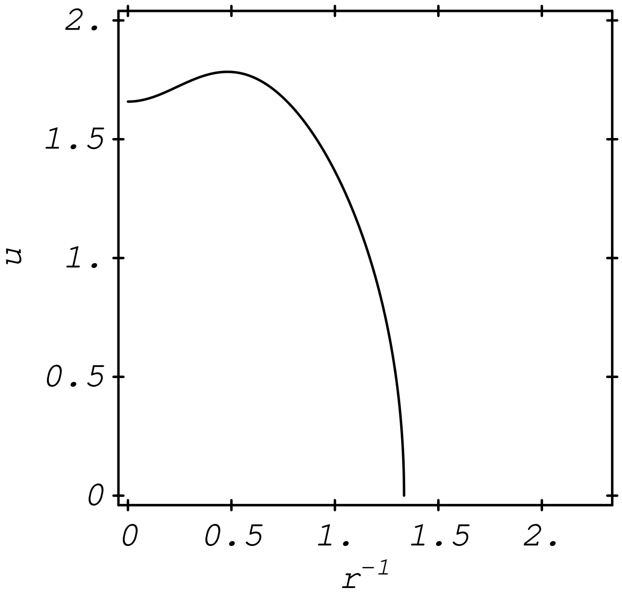


**Figure 6:** The curve of $dV_+/dr(r^{-1}, \mu) = 0$ for the parameter $n = 1$, $l = m = 1$, $j = 0$, and $a = 0.9$.

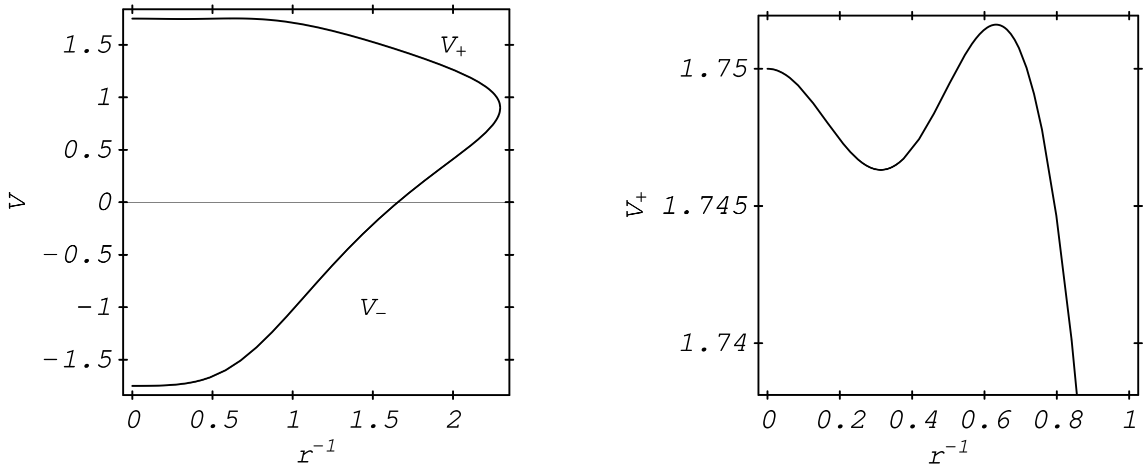


**Figure 7:** The factorized potentials $V_\pm$ as a function of $r^{-1}$. The potentials are characterized by $n = 1$, $l = m = 1$, $j = 0$, $\mu = 1.75$, and $a = 0.9$ (left panel). The right panel is the same as the left one, but, a close-up of the potential $V_+$ near extremes.


[4] Ya.B. Zel'dovich, *The generation of waves by a rotating body*, *Zh. Eksp. Teor. Fiz.* **14** (1971) 270 [*JETP Lett.* **14** (1971) 180]; *Zh. Eksp. Teor. Fiz.* **62** (1972) 2076 [*Sov. Phys. JETP* **35** (1972) 1085];
C.W. Misner, *Interpretation of gravitational-wave observations*, *Phys. Rev. Lett.* **28** (1972) 994;
J.D. Bekenstein, *Extraction of energy and charge from a black hole*, *Phys. Rev.* **D 7** (1973) 949;
W. Unruh, *Second quantization in the Kerr metric*, *Phys. Rev.* **D 10** (1974) 3194.

[5] W.H. Press and S.A. Teukolsky, *Floating orbits, superradiant scattering and the black-hole bomb*, *Nature* **238** (1972) 211.

[6] V. Cardoso, O.J.C. Dias, J.P.S. Lemos and S. Yoshida, *The black hole bomb and superradiant instabilities*, *Phys. Rev.* **D 70** (2004) 044039 [hep-th/0404096];
V. Cardoso and O.J.C. Dias, *Small kerr-anti-de Sitter black holes are unstable*, *Phys. Rev.* **D 70** (2004) 084011 [hep-th/0405006].

[7] T. Damour, N. Deruelle and R. Ruffini, *On quantum resonances in stationary geometries*, *Lett. Nuovo Cim.* **15** (1976) 257.

[8] T.M. Zouros and D.M. Eardley, *Instabilities of massive scalar perturbations of a rotating black hole*, *Ann. Phys. (NY)* **118** (1979) 139;
S. Detweiler, *Klein-gordon equation and rotating black holes*, *Phys. Rev.* **D 22** (1980) 2323;
H. Furuhashi and Y. Nambu, *Instability of massive scalar fields in Kerr-Newman spacetime*, *Prog. Theor. Phys.* **112** (2004) 983 [gr-qc/0402037];
M.J. Strafuss and G. Khanna, *Massive scalar field instability in Kerr spacetime*, *Phys. Rev.* **D 71** (2005) 024034 [gr-qc/0412023].

[9] R.C. Myers and M.J. Perry, *Black holes in higher dimensional space-times*, *Ann. Phys. (NY)* **172** (1986) 304.

[10] D.R. Brill, P.L. Chrzanowski, C. Martin Pereira, E.D. Fackerell and J.R. Ipser, *Solution of the scalar wave equation in a Kerr background by separation of variables*, *Phys. Rev.* **D 5** (1972) 1913;
S.A. Teukolsky, *Rotating black holes-separable wave equations for gravitational and electromagnetic perturbations*, *Phys. Rev. Lett.* **29** (1972) 1114.

[11] V.P. Frolov and D. Stojkovic, *Quantum radiation from a 5-dimensional rotating black hole*, *Phys. Rev.* **D 67** (2003) 084004 [gr-qc/0211055].

[12] M. Vasudevan, K.A. Stevens and D.N. Page, *Particle motion and scalar field propagation in Myers-Perry black hole spacetimes in all dimensions*, *Class. and Quant. Grav.* **22** (2005) 1469 [gr-qc/0407030].

[13] D. Ida, Y. Uchida and Y. Morisawa, *The scalar perturbation of the higher-dimensional rotating black holes*, *Phys. Rev.* **D 67** (2003) 084019 [gr-qc/0212035].

[14] E.W. Leaver, *An analytic representation for the quasi normal modes of Kerr black holes*, *Proc. R. Soc. London* **A402** (1985) 285.

[15] E.W. Leaver, *Quasinormal modes of Reissner-Nordström black holes*, *Phys. Rev.* **D 41** (1990) 2986.

[16] W. Gautschi, *Computational aspects of three-term recurrence relations*, *SIAM Rev.* **9** (1967) 24.

[17] W.H. Press, S.A. Teukolsky, W.T. Vetterling and B.P Flannery, *Numerical recipes: the art of scientific computing*, Cambridge University Press, Cambridge 1992.

[18] H.-P. Nollert, *Quasinormal modes of Schwarzschild black holes: the determination of quasinormal frequencies with very large imaginary parts*, *Phys. Rev.* **D 47** (1993) 5253.

[19] S.A. Teukolsky and W.H. Press, *Perturbations of a rotating black hole, III. Interaction of the hole with gravitational and electromagnetic radiation*, *Astrophys. J.* **193** (1974) 443.


JHEP07(2005)009

[20] F.R. Tangherlini, *Schwarzschild field in N dimensions and the dimensionality of space problem*, *Nuovo Cim.* **27** (1963) 636.

[21] V.P. Frolov and D. Stojkovic, *Particle and light motion in a space-time of a five-dimensional rotating black hole*, *Phys. Rev.* **D 68** (2003) 064011 [gr-qc/0301016].

[22] S. Yoshida, to be submitted.

[23] L.E. Simone and C.M. Will, *Massive scalar quasinormal modes of Schwarzschild and kerr black holes*, *Class. and Quant. Grav.* **9** (1992) 963.

[24] W.G. Unruh, *Experimental black hole evaporation*, *Phys. Rev. Lett.* **46** (1981) 1351.

[25] M. Visser, *Acoustic black holes: horizons, ergospheres and Hawking radiation*, *Class. and Quant. Grav.* **15** (1998) 1767 [gr-qc/9712010].

[26] E. Berti, V. Cardoso and J.P.S. Lemos, *Quasinormal modes and classical wave propagation in analogue black holes*, *Phys. Rev.* **D 70** (2004) 124006 [gr-qc/0408099];
V. Cardoso, J.P.S. Lemos and S. Yoshida, *Quasinormal modes and stability of the rotating acoustic black hole: numerical analysis*, *Phys. Rev.* **D 70** (2004) 124032 [gr-qc/0410107].

[27] S. Basak and P. Majumdar, *'Superresonance' from a rotating acoustic black hole*, *Class. and Quant. Grav.* **20** (2003) 3907 [gr-qc/0203059].

[28] J.L. Friedman, *Ergosphere instability*, *Commun. Math. Phys.* **63** (1978) 243;
N. Comins and B.F. Schutz, *On the ergoregion instability*, *Proc. R. Soc. Lond.* **A364** (1978) 211;
S. Yoshida and Y. Eriguchi, *Ergoregion instability revisited: a new and general method for numerical analysis of stability*, *MNRAS* **282** (1996) 580.

[29] H.S. Reall, *Classical and thermodynamic stability of black branes*, *Phys. Rev.* **D 64** (2001) 044005 [hep-th/0104071].

[30] S.S. Seahra, C. Clarkson and R. Maartens, *Detecting extra dimensions with gravity wave spectroscopy*, *Phys. Rev. Lett.* **94** (2005) 121302 [gr-qc/0408032];
see also E. Berti, K.D. Kokkotas and E. Papantonopoulos, *Gravitational stability of five-dimensional rotating black holes projected on the brane*, *Phys. Rev.* **D 68** (2003) 064020 [gr-qc/0306106].